

# Thin-shell wormholes in $N$ -dimensional $F(R)$ gravity

Griselda Figueroa-Aguirre<sup>1\*</sup>

<sup>1</sup> Instituto de Astronomía y Física del Espacio (IAFE, CONICET-UBA),  
Ciudad Universitaria, 1428 Buenos Aires, Argentina

## Abstract

In this work, spherically symmetric thin-shell wormholes with a conformally invariant Maxwell field for  $N$ -dimensional  $F(R)$  gravity and constant scalar curvature  $R$  are built. Two cases are considered: symmetric wormholes and asymmetric ones in the scalar curvature. Their stability under radial perturbations is analyzed, finding stable solutions made of exotic matter for a given range of the parameters.

## 1 Introduction

By adding terms to the gravitational Lagrangian, modified gravity theories have been proposed as alternatives to explain cosmological features such as the accelerated expansion of the universe or the early time inflation without resorting to exotic elements such as dark energy. Due to their relative simplicity, one of the most popular among them are the  $F(R)$  theories [1–3], which introduce a modification in the general relativity action by replacing the Ricci scalar  $R$  by a function  $F(R)$ . Many solutions in four dimensions have been found in this theory: among them, traversable wormholes [4–8] and spherically symmetric black holes [9–22]. Additional solutions have been explored in higher dimensions [23–26] as well as in lower ones [27]. Some of these solutions can be reduced to the black hole solutions in general relativity [28–34] within the adequate limits.

In the previous century, the Darmois–Israel formalism [35,36] has been developed as a technique which allows to craft a new manifold by cutting spacetimes and pasting them onto a hypersurface made of a thin layer of matter. In order to obtain a proper matching, certain particular conditions need to be fulfilled. Via the analysis of the energy–momentum tensor at this hypersurface, its stability can be analytically studied when it is done under perturbations that preserve the symmetry. Due to the popularity of this formalism, several applications of it can be found in the literature: for four-dimensional objects, one can list gravastars [37–39], bubbles [40], wormholes [41–46] and thin shells enclosing black holes [47–51], while for higher dimensions, thin shells of matter and wormholes [52–55].

Over the years, this formalism has been extended to other theories; in particular for  $F(R)$  gravity, a general set of junction conditions has been developed [56–58], showing that they have a more restrictive nature than those in general relativity. They always demand the continuity of the trace of the second fundamental form at the joining hypersurface. Depending on the third derivative of  $F(R)$ , the formalism branches out: for  $F'''(R) \neq 0$  the continuity of the scalar curvature  $R$  on the hypersurface is also demanded; if  $F'''(R) = 0$ , it is possible to construct spacetimes with a discontinuity of the scalar curvature across the hypersurface, in which case, extra contributions to the energy–momentum tensor appear in order to guarantee its local conservation [57,58]. Applications

---

\*e-mail: gfigueroa@iafe.uba.ar

of this formalism in  $F(R)$  gravity can be found in the literature; namely, thin shells and wormholes in four dimensions [59–66] as well as in lower dimensions [67, 68]. Thin shells in higher dimensional  $F(R)$  gravity have been analyzed [69], but there are no analogous studies with wormholes, hence, this motivates the present article to complete this topic in the literature.

In this work, spherically symmetric thin-shell wormholes with a conformally invariant Maxwell field for  $N$ -dimensional  $F(R)$  gravity are constructed. In Sects. 2 and 3, the general formalism and the procedure for the analysis of stability of static configurations under perturbations that preserve the symmetry are described. The generalized charged black hole solution with constant  $R$ , that is used for the construction of the wormholes, is shown in Sect. 4. Along Sect. 5, two examples of  $N$ -dimensional thin-shell wormholes are developed: symmetric and asymmetric ones. In Sect. 6, a summary of the work is presented. Along this article, the proper time derivative is denoted with a dot over a given quantity  $\Upsilon$ , that is,  $d\Upsilon/d\tau = \dot{\Upsilon}$ , while the radial derivative of the metric function  $A(r)$  is assigned with a prime, that is,  $dA(r)/dr = A'(r)$ . However, the prime on the  $F(R)$  describes the derivative with respect to the scalar curvature  $R$ , that is,  $dF(R)/dR = F'(R)$ . Units are taken such as  $c = G_N = 1$ , and the metric signature is  $(-, +, \dots, +)$ .

## 2 Wormhole construction

In order to construct a spherically symmetric wormhole in  $N$ -dimensional  $F(R)$  gravity, two metrics with the following form are adopted

$$ds^2 = -A_{1,2}(r)dt^2 + A_{1,2}(r)^{-1}dr^2 + r^2d\Omega^{N-2}, \quad d\Omega_{N-2}^2 = d\theta_1^2 + \sum_{i=2}^{N-2} \prod_{j=1}^{i-1} \sin^2 \theta_j d\theta_i^2, \quad (1)$$

where  $t$  is the time coordinate,  $r > 0$  is the radial coordinate,  $0 \leq \theta_i \leq \pi$  ( $1 \leq i \leq N-3$ ) and  $0 \leq \theta_{N-2} < 2\pi$  are the angular coordinates.

Two manifolds described by Eq. (1),  $\mathcal{M}_1$  and  $\mathcal{M}_2$  with constant scalar curvature  $R_{1,2}$ , are cut to  $r_{1,2} \geq a$ , with the radius  $a$  large enough in order to remove horizons and singularities, and paste them together onto a hypersurface  $\Sigma$  defined by  $G(r_{1,2}) = r_{1,2} - a = 0$ . Since these spaces are spherically symmetric, and the area of a  $(N-2)$ -sphere is proportional to  $r^{N-2}$ , it is always minimal for  $r = a$  so the flare-out condition is fulfilled, guaranteeing that the construction describes a wormhole with its throat at  $a$ . The new manifold  $\mathcal{M} = \mathcal{M}_1 \cup \mathcal{M}_2$  is the union of the previous ones, displaying different  $R_{1,2}$  at both sides of  $\Sigma$ . The coordinates of the original manifolds  $\mathcal{M}_{1,2}$  are  $X_{1,2}^\alpha = (t_{1,2}, r_{1,2}, \theta_1, \dots, \theta_{N-2})$ , and due to the spherical symmetry, the angular coordinates of each manifold have been mutually identified. Both coordinates,  $r_1$  in  $\mathcal{M}_1$  and  $r_2$  in  $\mathcal{M}_2$ , can be related to a new global radial coordinate in  $\mathcal{M}$  called  $\ell = \pm \int_a^{r_{1,2}} \sqrt{1/A_{1,2}(r_{1,2})} dr_{1,2}$ , where (+) sign corresponds to  $\mathcal{M}_1$  and (–) to  $\mathcal{M}_2$ , and  $\ell = 0$  is the position of the throat. On the hypersurface at  $a$ , the coordinates are  $\xi^i = (\tau, \theta_1, \dots, \theta_{N-2})$ , with  $\tau$  the proper time, which can be related to the coordinate time of the two manifolds through the expression

$$\frac{dt_{1,2}}{d\tau} = \frac{\sqrt{A_{1,2}(a) + \dot{a}^2}}{A_{1,2}(a)}, \quad (2)$$

where the signs are determined by choosing  $t_{1,2}$  and  $\tau$  to run into the direction of the future.

The first fundamental form for the original manifolds can be calculated as

$$h_{ij}^{1,2} = g_{\mu\nu}^{1,2} \frac{\partial X_{1,2}^\mu}{\partial \xi^i} \frac{\partial X_{1,2}^\nu}{\partial \xi^j} \Big|_{\Sigma}, \quad (3)$$

the extrinsic curvature or second fundamental form by

$$K_{ij}^{1,2} = -n_\gamma^{1,2} \left( \frac{\partial^2 X_{1,2}^\gamma}{\partial \xi^i \partial \xi^j} + \Gamma_{\alpha\beta}^\gamma \frac{\partial X_{1,2}^\alpha}{\partial \xi^i} \frac{\partial X_{1,2}^\beta}{\partial \xi^j} \right) \Big|_\Sigma, \quad (4)$$

where the unit normals ( $n^\gamma n_\gamma = 1$ ) are obtained via

$$n_\gamma^{1,2} = \left\{ \left| g_{1,2}^{\alpha\beta} \frac{\partial G}{\partial X_{1,2}^\alpha} \frac{\partial G}{\partial X_{1,2}^\beta} \right|^{-1/2} \frac{\partial G}{\partial X_{1,2}^\gamma} \right\} \Big|_\Sigma. \quad (5)$$

For an easy interpretation of the physical magnitudes, this construction is described by using the following orthonormal basis

$$e_{\hat{\tau}} = e_\tau, \quad e_{\hat{\theta}_1} = a^{-1} e_{\theta_1}, \quad e_{\hat{\theta}_i} = \left( a \prod_{j=1}^{i-1} \sin \theta_j \right)^{-1} e_{\theta_i} \quad \text{if } 2 \leq i \leq N-2.$$

When all these elements are calculated by using the metrics given by Eq. (1), the first fundamental form becomes

$$h_{ij}^{1,2} = \text{diag}(-1, 1, \dots, 1), \quad (6)$$

the unit normals read

$$n_\gamma^{1,2} = \pm \left( -\dot{a}, \frac{\sqrt{A_{1,2}(a) + \dot{a}^2}}{A_{1,2}(a)}, 0, \dots, 0 \right), \quad (7)$$

and the non-null components of the extrinsic curvature are given by

$$K_{\hat{\tau}\hat{\tau}}^{1,2} = \mp \frac{A'_{1,2}(a) + 2\ddot{a}}{2\sqrt{A_{1,2}(a) + \dot{a}^2}}, \quad (8)$$

and

$$K_{\hat{\theta}_i\hat{\theta}_i}^{1,2} = \pm \frac{1}{a} \sqrt{A_{1,2}(a) + \dot{a}^2}. \quad (9)$$

The junction formalism in  $F(R)$  gravity [57] requires the fulfillment of several conditions in order to obtain a proper matching hypersurface, namely

- The first fundamental form must be continuous at  $\Sigma$ , or in other words, the jump<sup>1</sup> of  $h_{\mu\nu}$  has to be zero,

$$[h_{\mu\nu}] = 0. \quad (10)$$

This condition is automatically satisfied in the current construction thanks to Eq. (6).

- The trace of the second fundamental form should be continuous at  $\Sigma$ ,

$$[K^\mu{}_\mu] = 0. \quad (11)$$

With the use of Eqs. (8) and (9), this condition can be translated to

$$\frac{2\ddot{a} + A'_2(a)}{2\sqrt{A_2(a) + \dot{a}^2}} + \frac{2\ddot{a} + A'_1(a)}{2\sqrt{A_1(a) + \dot{a}^2}} + \frac{(N-2)}{a} \left( \sqrt{A_2(a) + \dot{a}^2} + \sqrt{A_1(a) + \dot{a}^2} \right) = 0. \quad (12)$$

<sup>1</sup>Expressions within brackets such as  $[\Upsilon] \equiv (\Upsilon^2 - \Upsilon^1)|_\Sigma$  are used to define the jump of any quantity  $\Upsilon$  across the hypersurface  $\Sigma$ .

- A third condition may be required, depending on the value of the third derivative of  $F(R)$ . Here is where the formalism develops into two branches: when  $F'''(R) \neq 0$  [57, 58], the construction requires

$$[R] = 0. \quad (13)$$

However, this condition can be ignored if  $F'''(R) = 0$ . The way in which the formalism for the construction of a thin-shell wormhole branches out is explained in the following subsections.

## 2.1 Case $F'''(R) \neq 0$

When  $F'''(R) \neq 0$ , Eq.(13) should be satisfied and the field equations [57] at  $\Sigma$  take the form

$$\kappa S_{\mu\nu} = -F'(R)[K_{\mu\nu}] + F''(R)[\eta^\gamma \nabla_\gamma R]h_{\mu\nu}, \quad n^\mu S_{\mu\nu} = 0, \quad (14)$$

with  $\kappa = 8\pi$  and  $S_{\mu\nu}$  the energy-momentum tensor at  $\Sigma$ . When the scalar curvature is constant, this expression simplifies to

$$\kappa S_{\mu\nu} = -F'(R_0)[K_{\mu\nu}], \quad n^\mu S_{\mu\nu} = 0. \quad (15)$$

The energy-momentum tensor takes the diagonal form  $S_{ij} = \text{diag}(\sigma, p, \dots, p)$  in the orthonormal basis, with  $\sigma$  the hypersurface energy density and  $p \equiv p_{\hat{\theta}_i}$  ( $1 \leq i \leq N-2$ ) the transverse pressure. Their expressions read

$$\sigma = \frac{F'(R_0)}{\kappa} \left( \frac{2\ddot{a} + A'_2(a)}{2\sqrt{A_2(a) + \dot{a}^2}} + \frac{2\ddot{a} + A'_1(a)}{2\sqrt{A_1(a) + \dot{a}^2}} \right), \quad (16)$$

and

$$p = \frac{-F'(R_0)}{\kappa} \left( \frac{\sqrt{A_2(a) + \dot{a}^2}}{a} + \frac{\sqrt{A_1(a) + \dot{a}^2}}{a} \right). \quad (17)$$

With the help of Eqs. (16) and (17), Eq. (12) can be rewritten, resulting after some algebra, in the equation of state  $\sigma - (N-2)p = 0$ .

## 2.2 Case $F'''(R) = 0$

Due to  $F'''(R) = 0$ , it is easy to see that the construction is made within a quadratic  $F(R)$  theory, that is,  $F(R) = R - 2\Lambda + \gamma R^2$  and, therefore,  $F'(R) = 1 + 2\gamma R$ . For this particular case, the continuity of the scalar curvature given by the Eq. (13) is not necessary [57, 58]. The field equations [57] at  $\Sigma$  are given by

$$\kappa S_{\mu\nu} = -[K_{\mu\nu}] + 2\gamma([\eta^\gamma \nabla_\gamma R]h_{\mu\nu} - [RK_{\mu\nu}]), \quad n^\mu S_{\mu\nu} = 0. \quad (18)$$

However, when the scalar curvature  $R_{1,2}$  is constant at  $\Sigma$ , this expression can be simplified to

$$\kappa S_{\mu\nu} = -[K_{\mu\nu}] - 2\gamma[RK_{\mu\nu}], \quad n^\mu S_{\mu\nu} = 0. \quad (19)$$

In order to guarantee a divergence-free energy-momentum tensor, and therefore, local conservation, extra contributions are necessary. The energy-momentum tensor at  $\Sigma$  becomes  $(S_{\mu\nu} + \mathcal{T}n_\mu n_\nu + \mathcal{T}_\mu n_\nu + \mathcal{T}_\nu n_\mu)\delta^\Sigma + \mathcal{T}_{\mu\nu}$ , with  $\delta^\Sigma$  the Dirac delta on  $\Sigma$ , and

- $\mathcal{T}$  an external scalar pressure or tension

$$\kappa \mathcal{T} = 2\gamma[R]K^\gamma{}_\gamma, \quad (20)$$

- $\mathcal{T}_\mu$  an external energy flux vector,

$$\kappa\mathcal{T}_\mu = -2\gamma\bar{\nabla}_\mu[R] = 0, \quad n^\mu\mathcal{T}_\mu = 0, \quad (21)$$

where  $\bar{\nabla}$  the intrinsic covariant derivative on  $\Sigma$ . This element is zero when both  $R_{1,2}$  are constant.

- $\mathcal{T}_{\mu\nu}$  a two-covariant symmetric tensor distribution

$$\kappa\mathcal{T}_{\mu\nu} = \nabla_\beta \left( 2\gamma[R]h_{\mu\nu}n^\beta\delta^\Sigma \right), \quad (22)$$

which has a resemblance with classical dipole distributions.

For more details about these additional contributions, Refs. [57, 58] are recommended.

Once again, due to the use of the orthonormal basis, the energy-momentum tensor  $S_{ij} = \text{diag}(\sigma, p, \dots, p)$  has a diagonal form, allowing an easy identification with the physical magnitudes of the energy density  $\sigma$  and the pressure  $p$  on the hypersurface,

$$\sigma = \frac{1 + 2\gamma R_2}{\kappa} \left( \frac{2\ddot{a} + A'_2(a)}{2\sqrt{A_2(a) + \dot{a}^2}} \right) + \frac{1 + 2\gamma R_1}{\kappa} \left( \frac{2\ddot{a} + A'_1(a)}{2\sqrt{A_1(a) + \dot{a}^2}} \right), \quad (23)$$

and

$$p = -\frac{1 + 2\gamma R_2}{\kappa} \left( \frac{\sqrt{A_2(a) + \dot{a}^2}}{a} \right) - \frac{1 + 2\gamma R_1}{\kappa} \left( \frac{\sqrt{A_1(a) + \dot{a}^2}}{a} \right). \quad (24)$$

With Eq. (12) and (20), a symmetrical form of the external scalar pressure or tension  $\mathcal{T}$  can be written

$$\begin{aligned} \mathcal{T} = & \frac{2\gamma R_2}{\kappa} \left( \frac{2\ddot{a} + A'_2(a)}{2\sqrt{A_2(a) + \dot{a}^2}} + (N-2)\frac{\sqrt{A_2(a) + \dot{a}^2}}{a} \right) \\ & + \frac{2\gamma R_1}{\kappa} \left( \frac{2\ddot{a} + A'_1(a)}{2\sqrt{A_1(a) + \dot{a}^2}} + (N-2)\frac{\sqrt{A_1(a) + \dot{a}^2}}{a} \right). \end{aligned} \quad (25)$$

The tensor distribution  $\mathcal{T}_{ij}$  is proportional to  $2\gamma[R]h_{ij}/\kappa$ . Using Eqs. (23), (24), and (25), the expression of Eq. (12) can be rewritten, obtaining the equation of state  $\sigma - (N-2)p = \mathcal{T}$  for this case. The matter of the thin-shell wormhole can be characterized by using the weak energy condition (WEC); as long as it satisfies  $\sigma \geq 0$  and  $\sigma + p \geq 0$ , it is normal; otherwise it is exotic. Along this formalism, another requirement has been taken into consideration:  $F'(R) > 0$ , which is necessary within  $F(R)$  gravity to guarantee a positive effective Newton constant  $G_{eff} = G/F'(R_0)$ , and therefore, to avoid the presence of ghosts [70].

### 3 Stability analysis

For the stability analysis, radial perturbations of the static radius  $a_0$  of the throat are considered.

In all cases, the condition of the continuity of the trace of the second fundamental form given by Eq. (12) reduces to

$$\frac{A'_2(a_0)}{2\sqrt{A_2(a_0)}} + \frac{A'_1(a_0)}{2\sqrt{A_1(a_0)}} + \frac{(N-2)}{a_0} \left( \sqrt{A_2(a_0)} + \sqrt{A_1(a_0)} \right) = 0. \quad (26)$$

When  $F'''(R) \neq 0$ , the static values of the energy density  $\sigma_0$  and the pressure  $p_0$  are

$$\sigma_0 = \frac{F'(R_0)}{\kappa} \left( \frac{A'_2(a_0)}{2\sqrt{A_2(a_0)}} + \frac{A'_1(a_0)}{2\sqrt{A_1(a_0)}} \right), \quad (27)$$

and

$$p_0 = -\frac{F'(R_0)}{a_0\kappa} \left( \sqrt{A_2(a_0)} + \sqrt{A_1(a_0)} \right), \quad (28)$$

which give the equation of state  $\sigma_0 - (N-2)p_0 = 0$ .

For  $F'''(R) = 0$ , the energy density  $\sigma_0$ , pressure  $p_0$ , and external tension/pressure  $\mathcal{T}_0$  take the form

$$\sigma_0 = \frac{1 + 2\gamma R_2}{\kappa} \left( \frac{A'_2(a_0)}{2\sqrt{A_2(a_0)}} \right) + \frac{1 + 2\gamma R_1}{\kappa} \left( \frac{A'_1(a_0)}{2\sqrt{A_1(a_0)}} \right), \quad (29)$$

$$p_0 = -\frac{1 + 2\gamma R_2}{\kappa} \left( \frac{\sqrt{A_2(a_0)}}{a_0} \right) - \frac{1 + 2\gamma R_1}{\kappa} \left( \frac{\sqrt{A_1(a_0)}}{a_0} \right), \quad (30)$$

and

$$\mathcal{T}_0 = \frac{2\gamma R_2}{\kappa} \left( \frac{A'_2(a_0)}{2\sqrt{A_2(a_0)}} + (N-2) \frac{\sqrt{A_2(a_0)}}{a_0} \right) + \frac{2\gamma R_1}{\kappa} \left( \frac{A'_1(a_0)}{2\sqrt{A_1(a_0)}} + (N-2) \frac{\sqrt{A_1(a_0)}}{a_0} \right). \quad (31)$$

The equation of state now reads  $\sigma_0 - (N-2)p_0 = \mathcal{T}_0$ . The other non-null extra contribution is given by the double layer tensor distribution  $\mathcal{T}_{ij}^{(0)}$ , which is proportional to  $2\gamma(R_2 - R_1)h_{ij}/\kappa$ . For this case, a double layer of matter at the throat coexists with the thin shell.

To analyze the stability of these constructions under radial perturbations, it is useful to obtain an effective potential  $V(a)$  related to  $\dot{a}^2$  in the following form

$$\dot{a}^2 = -V(a). \quad (32)$$

The expression of Eq. (12) can be rewritten by considering  $\ddot{a} = (1/2)d(\dot{a}^2)/da$  and by using the definition  $z = \sqrt{A_2(a) + \dot{a}^2} - \sqrt{A_1(a) + \dot{a}^2}$ , obtaining

$$az'(a) + 2z(a) = 0. \quad (33)$$

Solving the differential equation above results in an expression for  $\dot{a}^2$  in terms of  $a$  and, therefore, for the potential in Eq. (32), which has the form

$$V(a) = -\frac{a_0^{2N-4} \left( \sqrt{A_2(a_0)} + \sqrt{A_1(a_0)} \right)^2}{4a^{2N-4}} + \frac{A_1(a) + A_2(a)}{2} - \frac{a^{2N-4} (A_2(a) - A_1(a))^2}{4a_0^{2N-4} \left( \sqrt{A_2(a_0)} + \sqrt{A_1(a_0)} \right)^2}. \quad (34)$$

This potential satisfies that  $V(a_0) = 0$  and, by using Eq. (26),  $V'(a_0) = 0$ . The second derivative

of Eq. (34) evaluated at the radius  $a_0$  gives

$$\begin{aligned}
V''(a_0) = & -\frac{(N-2)(2N-3)\left(\sqrt{A_2(a_0)} + \sqrt{A_1(a_0)}\right)^2}{2a_0^2} \\
& -\frac{(N-2)(2N-5)\left(\sqrt{A_2(a_0)} - \sqrt{A_1(a_0)}\right)^2}{2a_0^2} - \frac{(A_2'(a_0) - A_1'(a_0))^2}{2\left(\sqrt{A_2(a_0)} + \sqrt{A_1(a_0)}\right)^2} \\
& -\frac{2(N-2)(A_2(a_0) - A_1(a_0))(A_2'(a_0) - A_1'(a_0))}{a_0\left(\sqrt{A_2(a_0)} + \sqrt{A_1(a_0)}\right)^2} \\
& +\frac{A_1''(a_0) + A_2''(a_0)}{2} - \frac{(A_2(a_0) - A_1(a_0))(A_2''(a_0) - A_1''(a_0))}{2\left(\sqrt{A_1(a_0)} + \sqrt{A_2(a_0)}\right)^2}, \tag{35}
\end{aligned}$$

which determines that a static configuration is stable under radial perturbations when  $V''(a_0) > 0$ .

## 4 Black hole solutions with charge in $F(R)$ gravity

The action of  $F(R)$  gravity coupled to a power law non-linear electrodynamics reads [69]

$$I = \frac{1}{16\pi} \int d^n x \sqrt{-g} (R + f(R) - \alpha \varepsilon |\mathcal{F}|^s), \tag{36}$$

where  $R + f(R) = F(R)$  is the gravitational Lagrangian,  $\mathcal{F} = \mathcal{F}_{\alpha\beta}\mathcal{F}^{\alpha\beta}$  is the Maxwell invariant, and  $\mathcal{F}_{\mu\nu} = \partial_\mu\mathcal{A}_\nu - \partial_\nu\mathcal{A}_\mu$  is the electromagnetic tensor field in terms of the gauge potential  $\mathcal{A}_\mu$ . The constant  $s = N/4$  is adopted in order to have a traceless  $T_{\mu\nu}$ ,  $\alpha$  can be taken as 1 or  $-1$  depending on the Maxwell field considered, and  $\varepsilon = \text{sign}(\mathcal{F})$ .

For  $N \geq 4$ , constant scalar curvature  $R_0$ , and a purely radial electric field  $E(r) = F_{tr} = Q/r^2$ , the solution to the field equations obtained from Eq. (36) has the form given by Eq. (1), with the following metric function [69]

$$A(r) = 1 - \frac{2M}{r^{N-3}} + \frac{\alpha 2^{N/4} |Q|^{N/2}}{2(1 + f'(R_0))r^{N-2}} - \frac{R_0 r^2}{(N-1)N} \tag{37}$$

where  $Q$  is the electric charge and  $M$  the mass. It presents a singularity at  $r = 0$ , where Kretschmann scalar diverges. For  $\alpha = 1$ , there is a critical value of charge  $Q_c$ ; if  $|Q| \leq Q_c$  the solution presents an event horizon; for  $|Q| > Q_c$  has a naked singularity at the origin. The horizons are determined by the real, positive solutions of the equation  $A(r) = 0$ . For  $R_0 \leq 0$ , the event horizon is given by the largest one of them, while for  $R_0 > 0$ , the largest one corresponds to the cosmological horizon, and the second largest one to the event horizon. For  $\alpha = -1$ , there is no critical value of charge  $Q_c$  nor a naked singularity. In the same way as explained above, the event horizon is given by the largest real and positive solution of  $A(r) = 0$  when  $R_0 \leq 0$ . If  $R_0 > 0$ , the event horizon is determined by the second largest one while the largest one corresponds to the cosmological horizon.

The  $\hat{t}\hat{t}$ -component of the traceless energy-momentum tensor of the electromagnetic field associated with Eq. (36) can be expressed in the orthonormal coordinates by

$$T_{\hat{t}\hat{t}} = \frac{\alpha}{32\pi} 2^{N/4} |Q|^{N/2} (N-2), \tag{38}$$

which, for  $N \geq 3$ , is positive if  $\alpha > 0$  or negative if otherwise. Since wormholes are constructed in the present work, and they allow the presence of exotic matter, the parameter  $\alpha$  is left free to analyze its effect.

## 5 Examples

Two examples of thin-shell wormholes using the geometry (1), with the metric function given by Eq. (37), are presented. To do so, a general spacetime  $\mathcal{M}$  is constructed by cutting and pasting two regions:  $\mathcal{M}_1$  and  $\mathcal{M}_2$ . The result of this process is a thin layer of matter which static radius  $a_0$  is always solution of Eq. (11) and determines the throat of a wormhole by fulfilling the flare-out condition. Its stability under radial perturbations is given by the sign of the second derivative of the effective potential (35).

In order to show the results, the most representative graphics have been chosen for Fig. 1, 2, 3, 4 5, and 6. In them, the solid lines represent the stable solutions, the dashed lines the unstable ones, the meshed regions indicate where the WEC condition is satisfied (and therefore the solution is made of normal matter) and the grey regions lack of physical meaning. Since the increase of the dimensionality of the spacetime only offers a change of scale without altering the qualitative behavior of the solutions, the graphical presentation of the results is limited to  $N = 5$  and  $N = 4$  (the dimensionality  $N = 4$  is included for comparison). The construction has been explored by using  $\alpha = 1$  and  $\alpha = -1$  as well. In order to prevent the presence of ghosts, this work follows the condition of  $F'(R) > 0$ , for further details, Ref. [70] is suggested.

### 5.1 Symmetric wormholes

For the construction of this type of wormhole, the metric function given by Eq. (37) is taken the same at both sides of the throat, this is,  $A_1(a) = A_2(a)$ , or equivalently, with  $M_1 = M_2 = M$ ,  $Q_1 = Q_2 = Q$ , and  $R_1 = R_2 = R_0$ . The static radius of the throat  $a_0$  has to be larger than the event horizon and smaller than the cosmological one when it exists. For both values of  $\alpha$  there is always a radial electric field  $E(r) = F_{tr} = Q/r^2$ .

The results for a symmetric wormhole with  $\alpha = 1$  are shown in Fig. 1, where the columns are related to the dimension of the spacetime, that is,  $N = 4$  and  $N = 5$ , while the rows correspond to different values of the constant scalar curvature  $R_0$ . Variations in the mass  $M$  of the construction only alter its scale; therefore, all quantities have been adimensionalized with  $M$ . The meshed regions represent the areas where the WEC condition is fulfilled. For this particular case in Fig. 1, the first row shows the results of  $R_0 M^{2/(N-3)} = 0.4$  and the second one of  $R_0 M^{2/(N-3)} = -0.4$ . Due to the difficulty in seeing the behavior of the solutions around the  $Q_c$  because the scale of the graphics, Fig. 2 has been added. It is a zoom-in of the region around  $Q_c$  for the particular case of  $R_0 M^{2/(N-3)} = 0.4$ . The behavior displayed in it is similar for all the cases presented in Fig. 1. For  $\alpha = -1$ , the results can be seen in Fig. 3. For this case, only  $R_0 > 0$  has been considered, since there is no solution of Eq. (26) for  $R_0 \leq 0$  (they are inside the grey region). The figure shows in its first row the results for  $R_0 M^{2/(N-3)} = 0.2$  and in the second row for  $R_0 M^{2/(N-3)} = 0.1$ . The results can be summarized in the following list

- For  $\alpha = 1$ 
  - When  $R_0 > 0$  and  $|Q| \leq Q_c$ , there is one unstable solution made of exotic matter close to the cosmological horizon. For  $|Q| \gtrsim Q_c$ , and for a small range of values of charge, there are three solutions made of exotic matter: one of them is stable. For large values of  $|Q|$  there is only one unstable solution made of exotic matter.



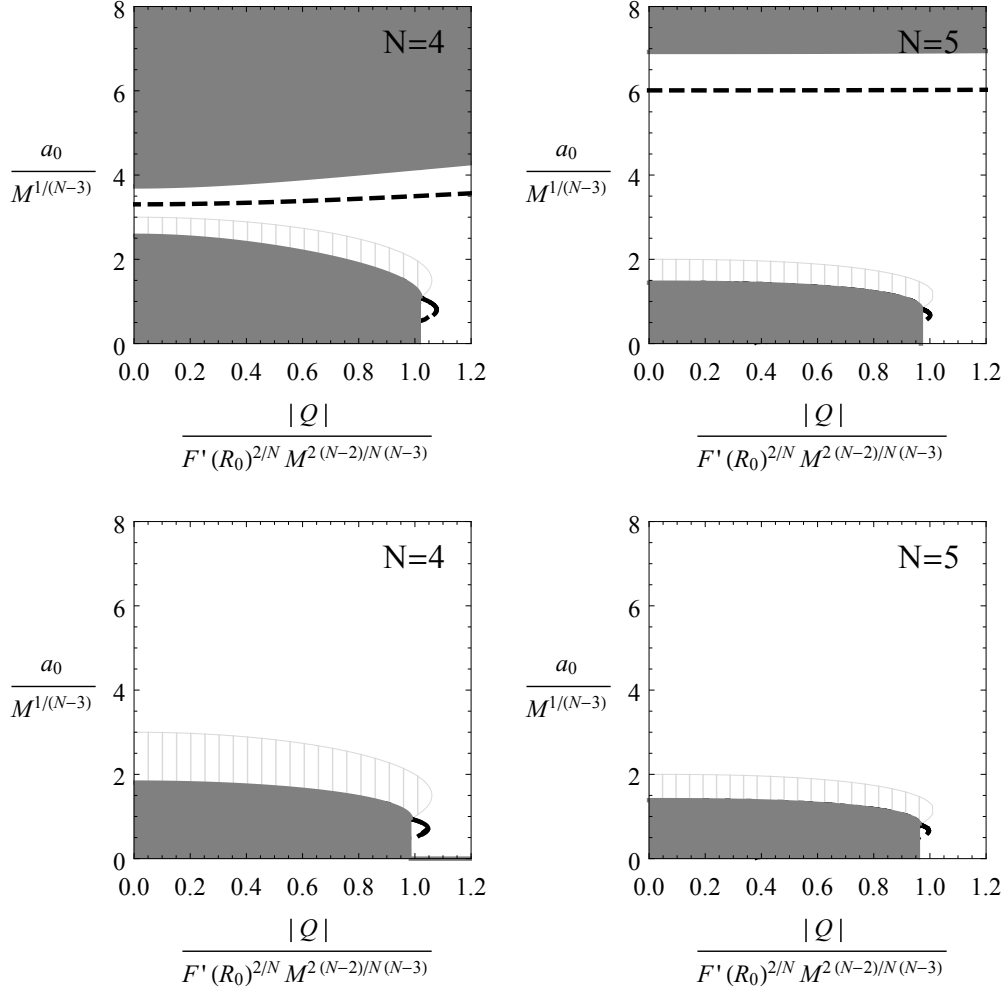


Figure 1: Wormholes with  $R_1 = R_2 = R_0$  and  $\alpha = 1$ . The first column shows the results for  $N = 4$ , while the second one for  $N = 5$ . Stable configurations are displayed by solid lines and unstable ones by dashed lines. Meshed regions are related to normal matter, grey zones have no physical meaning. The first row corresponds to plots with  $R_0 M^{2/(N-3)} = 0.4$  and the second row with  $R_0 M^{2/(N-3)} = -0.4$ .

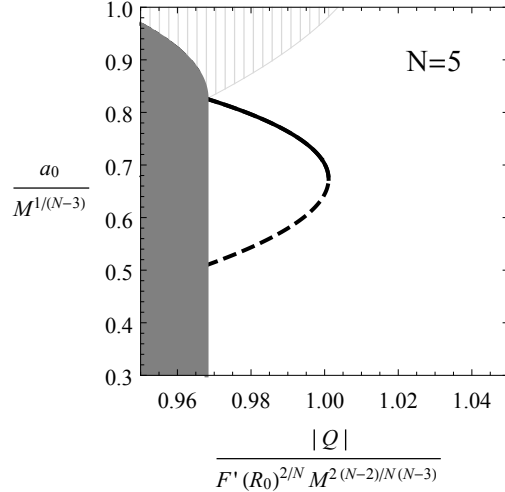


Figure 2: Zoom-in of the region around the value  $Q_c$  for wormholes with  $\alpha = 1$ ,  $N = 5$  and  $R_0 M^{2/(N-3)} = 0.4$  shown in Fig. 1. This behavior is analogous for the rest of the plots displayed in that figure.

- When  $R_0 \leq 0$  there are only two solutions for a short range of charge  $|Q| \gtrsim Q_c$ . These solutions are made of exotic matter; the smaller one is unstable while the larger one is stable.
- The qualitative behavior of the solutions changes with the sign of the scalar curvature  $R_0$ .
- The behavior of the solutions do not change with the increase of the dimension  $N$ . It only produces a change of scale.
- For  $\alpha = -1$ 
  - Physical solutions are only possible for  $R_0 > 0$ .
  - When  $R_0 > 0$  there is only one unstable solution made of exotic matter, always close to the cosmological horizon.
  - The qualitative behavior of the solution changes with the sign of  $R_0$ . Variations in its dimensionality  $N$  only cause a change of scale.
- The equation of state for symmetric wormholes is  $\sigma_0 - (N - 2)p_0 = 0$ .

## 5.2 Asymmetric wormholes

For the case asymmetric in the scalar curvature, quadratic theories are considered, which allow the relaxation of the continuity of  $R_{1,2}$  expressed in Eq. (13). The function metric for this construction is then given by Eq. (37) with  $M_1 = M_2 = M$  and  $Q_1 = Q_2 = Q$ , but different constant values of  $R_1 \neq R_2$  across the throat

$$A_{1,2}(r) = 1 - \frac{2M}{r^{N-3}} + \frac{\alpha 2^{N/4} |Q|^{N/2}}{2(1 + 2\gamma R_{1,2}) r^{N-2}} - \frac{R_{1,2} r^2}{(N-1)N}. \quad (39)$$

Proceeding in the same fashion as it was done in the previous section, the radius of the throat  $a_0$ , which is solution of the Eq. (26), has to be larger than the event horizon and, when  $R_{1,2} > 0$ , smaller than the cosmological one.

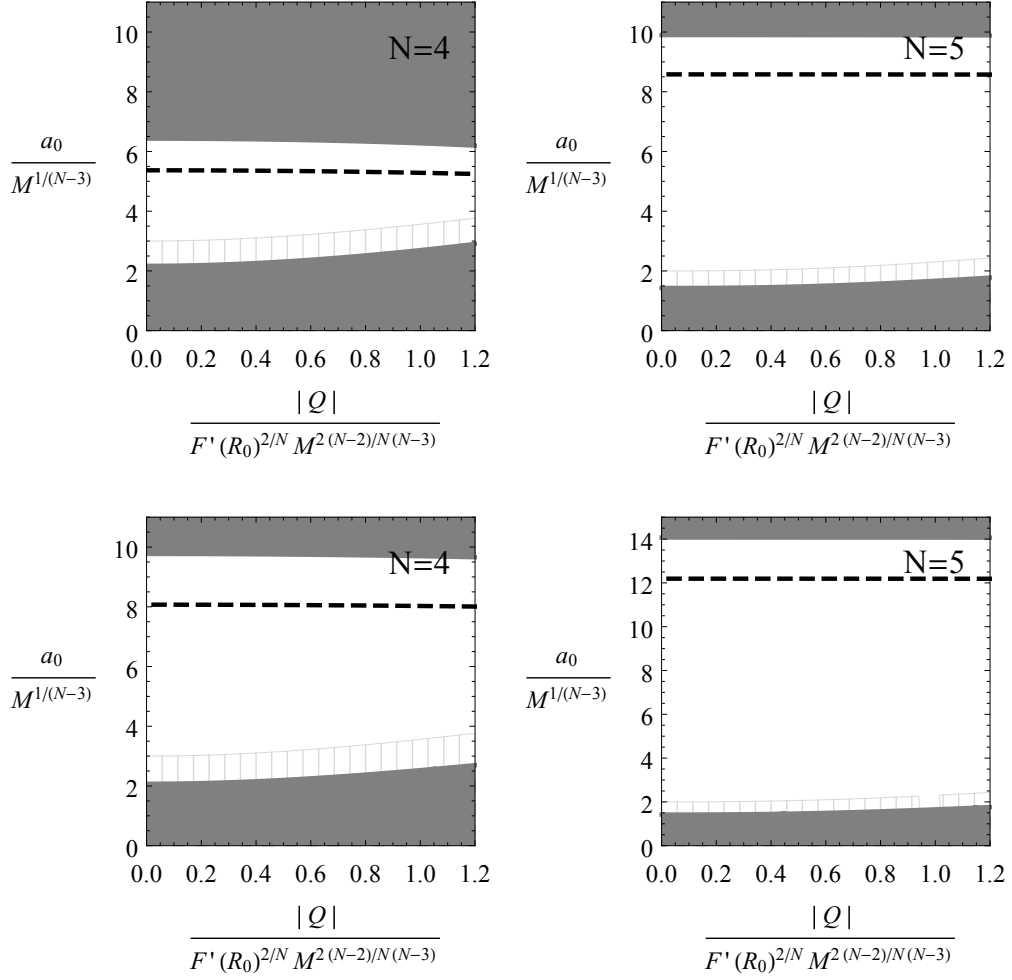


Figure 3: Wormholes with  $R_1 = R_2 = R_0$  and  $\alpha = -1$ . The meaning of  $N$ , the solid and dashed lines, and the grey and meshed regions are the same as in Fig. 1. The first row corresponds to the plots with  $R_0 M^{2/(N-3)} = 0.2$  and the second row with  $R_0 M^{2/(N-3)} = 0.1$ .

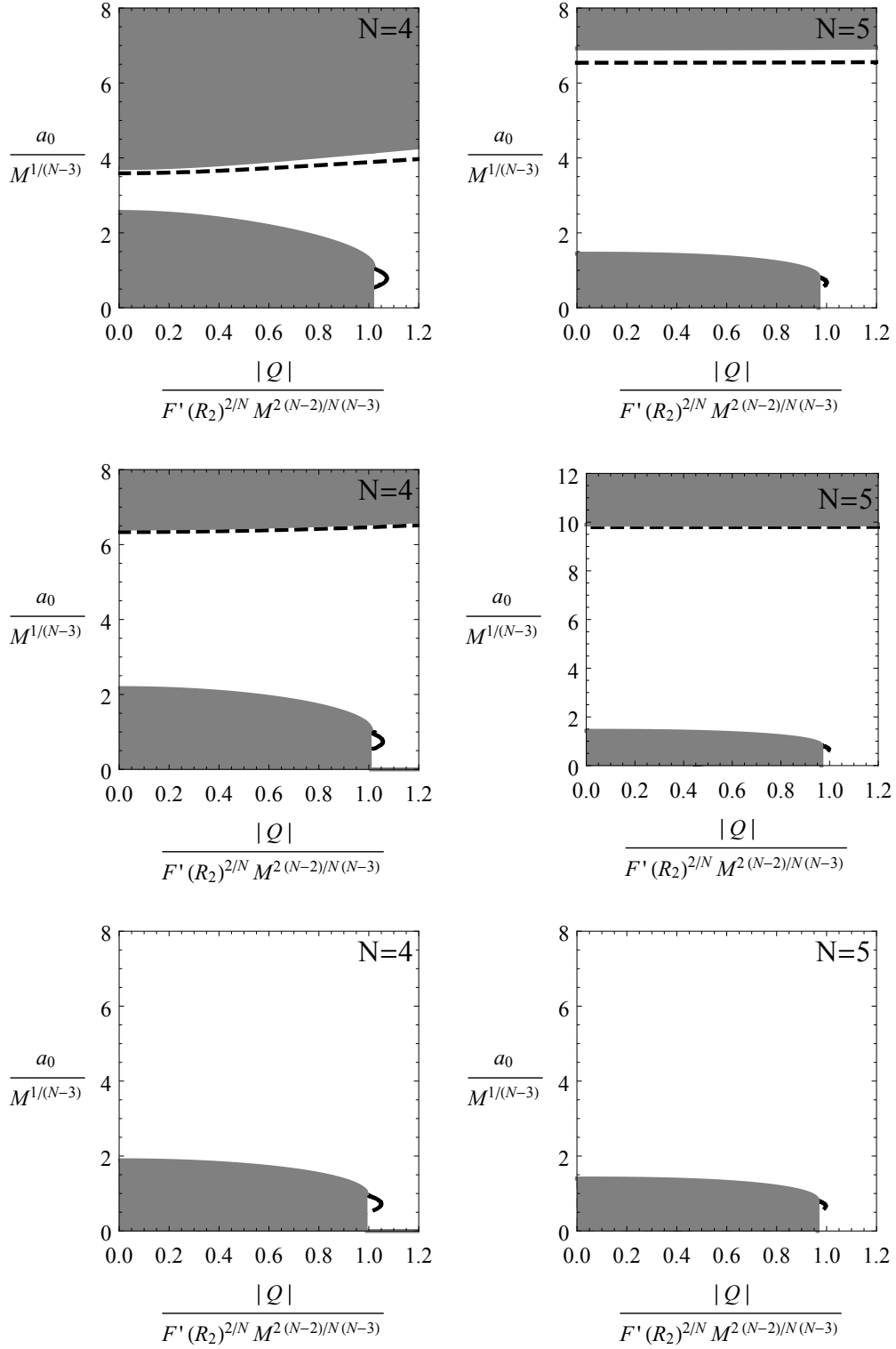


Figure 4: Wormholes with  $R_1 \neq R_2$ ,  $\gamma/M = 0.1$ , and  $\alpha = 1$ . The meaning of  $N$ , the solid and dashed lines, and the grey regions are the same as in Fig.1. The first row corresponds to  $R_1 M^{2/(N-3)} = 0.2$  and  $R_2 M^{2/(N-3)} = 0.4$ , the second row to  $R_1 M^{2/(N-3)} = 0.2$  and  $R_2 M^{2/(N-3)} = -0.4$ , and the third row to  $R_1 M^{2/(N-3)} = -0.2$  and  $R_2 M^{2/(N-3)} = -0.4$ .

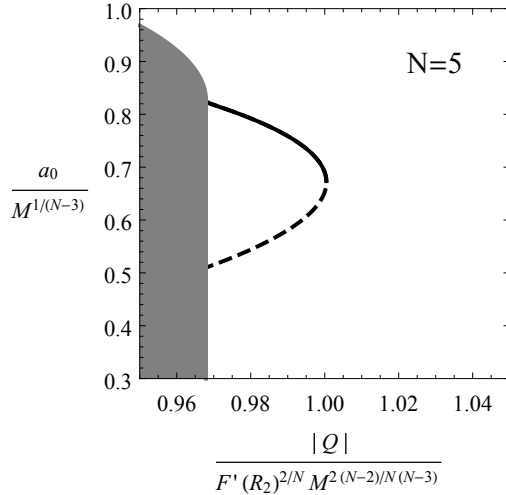


Figure 5: Zoom-in of the region around the value  $Q_c$  for wormholes with  $\alpha = 1$ ,  $\gamma/M = 0.1$ ,  $N = 5$ ,  $R_1 M^{2/(N-3)} = 0.2$  and  $R_2 M^{2/(N-3)} = 0.4$  shown in Fig. 4. This behavior is analogous for the rest of the cases displayed in that figure.

The plots show the results for  $R_1 \neq R_2$ ; the columns display the dimension, and the rows different combinations of the values of  $R_1$  and  $R_2$ . All quantities have been adimensionalized with  $M$ , and  $\gamma/M = 0.1$  has been taken. The solid and dashed curves, the meshed zones, and the grey regions keep the same interpretation as before. The graphics in Fig. 4 has been done with  $\alpha = 1$ ; the first row corresponds to  $R_1 M^{2/(N-3)} = 0.2$  and  $R_2 M^{2/(N-3)} = 0.4$ , the second row to  $R_1 M^{2/(N-3)} = 0.2$  and  $R_2 M^{2/(N-3)} = -0.4$ , and the third row to  $R_1 M^{2/(N-3)} = -0.2$  and  $R_2 M^{2/(N-3)} = -0.4$ . Because the similar qualitative behavior of the solution around  $Q_c$ , Fig. 5 has been added to better see the details despite the scale. It displays the case for  $N = 5$ ,  $R_1 M^{2/(N-3)} = 0.2$ , and  $R_2 M^{2/(N-3)} = 0.4$ . The plots in Fig. 6 are for  $\alpha = -1$ , and present different combinations of  $R_{1,2}$  except for  $R_1 < 0$  and  $R_2 < 0$ , in which case there is no physical solution. The columns display the dimensionality of the construction, the first row corresponds to  $R_1 M^{2/(N-3)} = 0.2$  and  $R_2 M^{2/(N-3)} = 0.1$ , and the second row to  $R_1 M^{2/(N-3)} = 0.2$  and  $R_2 M^{2/(N-3)} = -0.1$ . The results can be listed as

- For  $\alpha = 1$ 
  - When  $R_1 > 0$  and  $R_2 > 0$ , or  $R_1 R_2 < 0$ , and  $|Q| \leq Q_c$ , there is only one unstable solution composed of exotic matter. For a small range of values of charges  $|Q| \gtrsim Q_c$ , there are three solutions composed of exotic matter; two of them unstable, and only one stable. For large values of  $|Q|$  only one unstable solution made of exotic matter can be found.
  - When  $R_1 < 0$  and  $R_2 < 0$ , two solutions made of exotic matter are found for a short range of charge  $|Q| \gtrsim Q_c$ . The larger one is stable.
  - The sign combination in  $R_1$  and  $R_2$  modifies the qualitative behavior of the solutions.
  - Increasing the dimensionality of the construction does not change the behavior of the solutions, only its scale.
- For  $\alpha = -1$ 
  - For  $R_1 < 0$  and  $R_2 < 0$ , physical solutions do not exist.

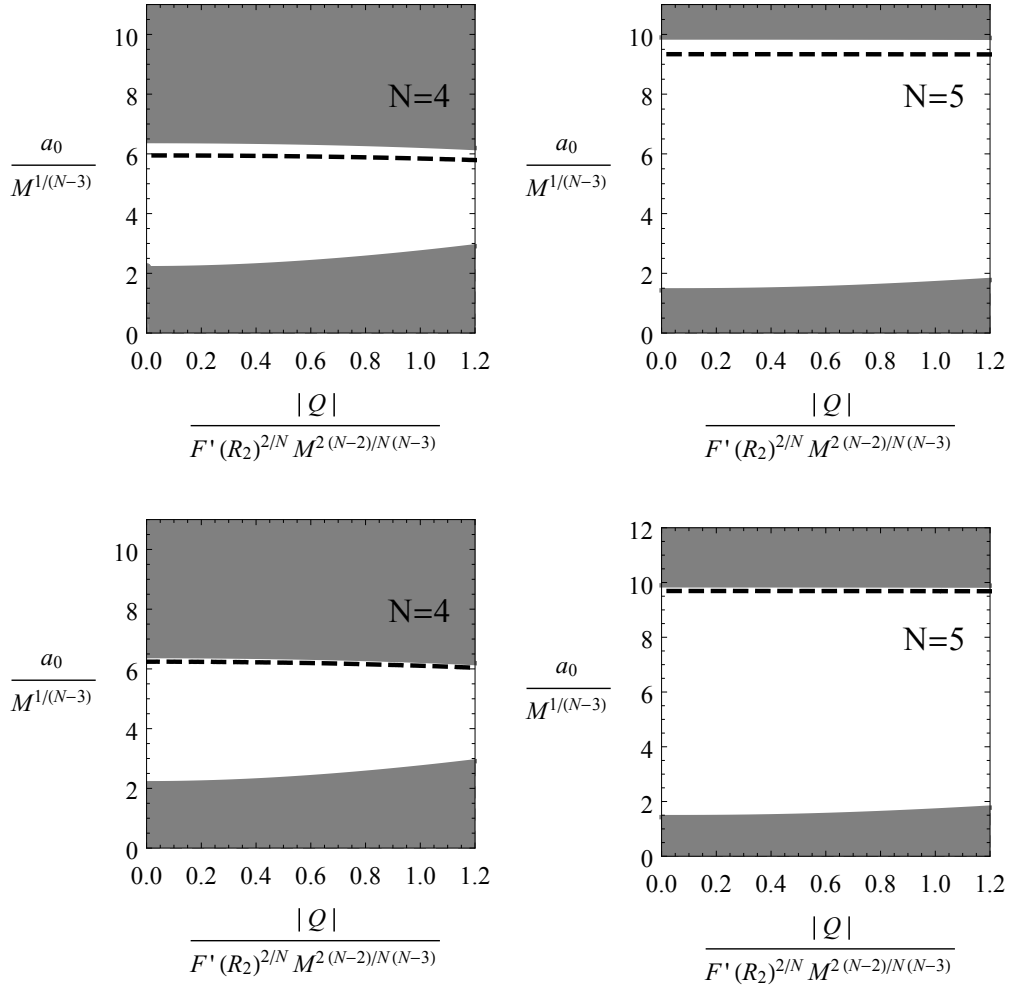


Figure 6: Wormholes with  $R_1 \neq R_2$ ,  $\gamma/M = 0.1$ , and  $\alpha = -1$ . The meaning of  $N$ , the solid and dashed lines, and the grey regions are the same as in Fig. 1. The first row corresponds to  $R_1 M^{2/(N-3)} = 0.2$  and  $R_2 M^{2/(N-3)} = 0.1$ , and the second row to  $R_1 M^{2/(N-3)} = 0.2$  and  $R_2 M^{2/(N-3)} = -0.1$ .

- For the rest of combinations of  $R_1$  and  $R_2$ , only one unstable solution made of exotic matter, close to the cosmological horizon, is found.
- The qualitative behavior of the solutions changes with the sign combination of  $R_1$  and  $R_2$ , while the dimensionality  $N$  only produces a change of scale.
- For both values of  $\alpha$ , the external energy flux vector  $\mathcal{T}_\mu$ , given by Eq. (21), is zero, and the tensor distribution  $\mathcal{T}_{ij}$  is proportional to  $2\gamma(R_2 - R_1)h_{ij}/\kappa$ . Therefore, the thin shell of matter that constitutes the throat coexists with a double layer.
- The equation of state for asymmetric wormholes in quadratic  $F(R)$  theories has the form  $\sigma - (N - 2)p = \mathcal{T}$ .

## 6 Summary

In this work, a family of wormholes have been built by using a generalized spherical symmetric black hole solution with constant scalar curvature  $R$  for  $N$ -dimensional  $F(R)$  gravity coupled to a conformally invariant Maxwell field. The stability of the static configurations under radial perturbations has been studied, keeping into consideration  $F'(R) > 0$  to prevent the presence of ghosts.

Two examples of wormholes have been given, showing the formalism of the construction for  $N \geq 4$ , a purely radial electromagnetic field with charge  $Q$ , and a traceless energy-momentum tensor. The two different values  $\alpha = 1$  and  $\alpha = -1$  have been explored in each of them. The first example has been constructed within a general  $F(R)$ , in which case the formalism demands to keep the same value of the constant scalar curvature  $R_0$  across the throat. The second example is built within a quadratic  $F(R)$  theory, allowing different values of the constant scalar curvature  $R_1 \neq R_2$ . In both cases, the expressions of the energy density  $\sigma$  and the pressure  $p$  at the throat, as well as the equation of state they satisfy, have been found. For quadratic  $F(R)$ , the usual extra contributions that appear in the theory when  $R_1 \neq R_2$  have been also shown. In each scenario, the stability of the static configurations for a radius  $a_0$  and different combination of the parameters have been analyzed.

In order to construct a symmetric wormhole within a general  $F(R)$  theory, the same mass, charge, and constant scalar curvature  $R_0$  at both sides of the throat have been used. For  $\alpha = -1$  only unstable solutions are found, while for  $\alpha = 1$ , there are stable solutions for a short range of values of the charge. For both values of  $\alpha$ , they are always made of exotic matter. The behavior of the solutions depends on the sign of  $R_0$  independently of their dimensionality, which only changes their scale.

For the case of quadratic  $F(R)$ , different constant scalar curvatures  $R_1 \neq R_2$  have been used. If both of them  $R_{1,2}$  are negative, there are no physical solutions. In similar way to the previous case, for  $\alpha = -1$  only unstable solutions made of exotic matter can be found. For  $\alpha = 1$  and a short range of values of the charge, there is a stable solution, which is also made of exotic matter. The behavior of the solutions changes with the relative sign between  $R_1$  and  $R_2$ , while the dimensionality of the construction  $N$  only changes its scale.

## Acknowledgments

The author thanks to Ernesto F. Eiroa for his useful comments. This work has been supported by CONICET and Universidad de Buenos Aires.

## References

- [1] T.P. Sotiriou and V. Faraoni, *Rev. Mod. Phys.* **82**, 451 (2010).
- [2] A. De Felice and S. Tsujikawa, *Living Rev. Relativity* **13**, 3 (2010).
- [3] S. Nojiri, S.D. Odintsov, and V.K. Oikonomou, *Phys. Rep.* **692**, 1 (2017).
- [4] A. DeBenedictis and D. Horvat, *Gen. Relativ. Gravit.* **44**, 2711 (2012).
- [5] T. Harko, F.S.N. Lobo, M.K. Mak, and S.V. Sushkov, *Phys. Rev. D* **87**, 067504 (2013).
- [6] J.L. Rosa, J.P.S. Lemos, and F.S.N. Lobo, *Phys. Rev. D* **98**, 064054 (2018).
- [7] H. Golchin and M.R. Mehdizadeh, *Eur. Phys. J. C* **79**, 777 (2019).
- [8] F.S.N. Lobo, G.J. Olmo, E. Orazi, D. Rubiera-Garcia, and A. Rustam, *Phys. Rev. D* **102**, 104012 (2020).
- [9] T. Multamäki and I. Vilja, *Phys. Rev. D* **74**, 064022 (2006).
- [10] S. Capozziello, A. Stabile, and A. Troisi, *Class. Quantum Gravity* **25**, 085004 (2008).
- [11] A. de la Cruz-Dombriz, A. Dobado, and A.L. Maroto, *Phys. Rev. D* **80**, 124011 (2009); **83**, 029903(E) (2011).
- [12] T. Moon, Y.S. Myung, and E.J. Son, *Gen. Relativ. Gravit.* **43**, 3079 (2011).
- [13] S. H. Hendi and D. Momeni, *Eur. Phys. J. C* **71**, 1823 (2011).
- [14] G. G. L. Nashed and S. Nojiri, *Phys. Rev. D* **104**, 124054 (2021).
- [15] T. Karakasis, E. Papantonopoulos, Z.Y. Tang, and B. Wang, *Eur. Phys. J. C* **81**, 897 (2021).
- [16] L. Sebastiani and S. Zerbini, *Eur. Phys. J. C* **71**, 1591 (2011).
- [17] S. Habib Mazharimousavi, M. Halilsoy, and T. Tahamtan, *Eur. Phys. J. C* **72**, 1851 (2012).
- [18] P. Cañate, L.G. Jaime, and M. Salgado, *Class. Quantum Grav.* **33**, 155005 (2016).
- [19] P. Cañate, *Class. Quantum Grav.* **35**, 025018 (2018).
- [20] E. Elizalde, G.G.L. Nashed, S. Nojiri, and S.D. Odintsov, *Eur. Phys. J. C* **80**, 109 (2020).
- [21] G. G. L. Nashed and S. Nojiri, *Phys. Rev. D* **102**, 124022 (2020).
- [22] G. G. L. Nashed and S. Nojiri, *Phys. Lett. B* **820**, 136475 (2021).
- [23] S.H. Hendi, *Phys. Lett. B* **690**, 220 (2010).
- [24] S.H. Hendi, B. Eslam Panah, and S.M. Mousavi, *Gen. Relativ. Gravit.* **44**, 835 (2012).
- [25] A. Sheykhi, *Phys. Rev. D* **86**, 024013 (2012).
- [26] Z.Y. Tang, B. Wang, and E. Papantonopoulos, *Eur. Phys. J. C* **81**, 346 (2021).
- [27] S.H. Hendi, B. Eslam Panah, and R. Saffari, *Int. J. Mod. Phys. D* **23**, 1450088 (2014).



- [28] M. Hassaïne and C. Martínez, *Phys. Rev. D* **75**, 027502 (2007).
- [29] M. Hassaïne and C. Martínez, *Class. Quantum Grav.* **25**, 195023 (2008).
- [30] S. Habib Mazharimousavi, *Class. Quantum Grav.* **37**, 197001 (2020).
- [31] D. Kokoška and M. Ortaggio, *Phys. Rev. D* **104**, 124051 (2021).
- [32] M. Cataldo, N. Cruz, S. del Campo, and A. García, *Phys. Lett. B*, **484**, 154 (2000).
- [33] O. Gurtug, S. Habib Mazharimousavi, and M. Halilsoy, *Phys. Rev. D* **85**, 104004 (2012).
- [34] M. Bañados, C. Teitelboim, and J. Zanelli, *Phys. Rev. Lett.* **69**, 1849 (1992).
- [35] G. Darmois, *Mémoires des Sciences Mathématiques, Fascicule XXV, Chap. V* (Gauthier-Villars, Paris, 1927).
- [36] W. Israel, *Nuovo Cimento B* **44**, 1 (1966); **48**, 463(E) (1967).
- [37] M. Visser and D.L. Wiltshire, *Class. Quantum Gravity* **21**, 1135 (2004).
- [38] F. S. N. Lobo and A. V. B. Arellano, *Class. Quantum Gravity* **24**, 1069 (2007).
- [39] P. Martin-Moruno, N. Montelongo Garcia, F.S.N. Lobo, and M. Visser, *J. Cosmol. Astropart. Phys.* **03**, 034 (2012).
- [40] V.A. Berezin, V.A. Kuzmin, and I.I. Tkachev, *Phys. Rev. D* **36**, 2919 (1987).
- [41] E. Poisson and M. Visser, *Phys. Rev. D* **52**, 7318 (1995).
- [42] E.F. Eiroa and G.E. Romero, *Gen. Relativ. Gravit.* **36**, 651 (2004).
- [43] E.F. Eiroa, *Phys. Rev. D* **78**, 024018 (2008).
- [44] N. Montelongo Garcia, F.S.N. Lobo, and M. Visser, *Phys. Rev. D* **86**, 044026 (2012).
- [45] S.D. Forghani, S. Habib Mazharimousavi, and M. Halilsoy, *Eur. Phys. J. C* **78**, 469 (2018).
- [46] T. Berry, F.S.N. Lobo, A. Simpson, and M. Visser, *Phys. Rev. D* **102**, 064054 (2020).
- [47] P.R. Brady, J. Louko and E. Poisson, *Phys. Rev. D* **44**, 1891 (1991).
- [48] M. Ishak and K. Lake, *Phys. Rev. D* **65**, 044011 (2002).
- [49] F.S.N. Lobo and P. Crawford, *Class. Quantum Gravity* **22**, 4869 (2005).
- [50] E.F. Eiroa and C. Simeone, *Phys. Rev. D* **83**, 104009 (2011).
- [51] M. Sharif and S. Iftikhar, *Astrophys. Space Sci.* **356**, 89 (2015).
- [52] G.A.S. Dias and J.P.S. Lemos, *Phys. Rev. D* **82**, 084023 (2010).
- [53] F. Rahaman, M. Kalam, and S. Chakraborty, *Gen. Relativ. Gravit.* **38**, 1687 (2006).
- [54] A. Banerjee, K. Jusufi, and S. Bahamonde, *Grav. Cosmol.* **24**, 71 (2018).
- [55] E.F. Eiroa and C. Simeone, *Int. J. Mod. Phys. D* **21**, 1250033 (2012).

- [56] N. Deruelle, M. Sasaki, and Y. Sendouda, *Prog. Theor. Phys.* **119**, 237 (2008).
- [57] J.M.M. Senovilla, *J. Phys. Conf. Ser.* **600**, 012004 (2015)
- [58] B. Reina, J.M.M. Senovilla, and R. Vera, *Class. Quantum Gravity* **33**, 105008 (2016).
- [59] E.F. Eiroa and G. Figueroa-Aguirre, *Eur. Phys. J. C* **76**, 132 (2016).
- [60] E.F. Eiroa and G. Figueroa-Aguirre, *Phys. Rev. D* **94**, 044016 (2016).
- [61] M. Zaeem-ul-Haq Bhatti, A. Anwar, and S. Ashraf, *Mod. Phys. Lett. A* **32**, 1750111 (2017).
- [62] S. Habib Mazharimousavi, *Eur. Phys. J. C* **78**, 612 (2018).
- [63] S. Habib Mazharimousavi, M. Halilsoy, and K. Kianfar, *Eur. Phys. J. Plus* **135**, 440 (2020).
- [64] E.F. Eiroa, G. Figueroa-Aguirre, and J.M.M. Senovilla, *Phys. Rev. D* **95**, 124021 (2017).
- [65] E.F. Eiroa and G. Figueroa-Aguirre, *Eur. Phys. J. C* **78**, 54 (2018).
- [66] E.F. Eiroa and G. Figueroa-Aguirre, *Eur. Phys. J. C* **79**, 171 (2019).
- [67] E. F. Eiroa and G. Figueroa-Aguirre, *Phys. Rev. D* **103**, 044011 (2021)
- [68] C. Bejarano, E. F. Eiroa, and G. Figueroa-Aguirre, *Eur. Phys. J. C* **81**, 668 (2021).
- [69] E. F. Eiroa and G. Figueroa-Aguirre, *Eur. Phys. J. Plus* **137**, 478 (2022).
- [70] K.A. Bronnikov, M.V. Skvortsova, and A.A. Starobinsky, *Grav. Cosmol.* **16**, 216 (2010).